学位論文

Formation of *N*-acyl-phosphatidylethanolamines by cytosolic phospholipase $A_2\varepsilon$ in an ex vivo murine model of brain ischemia

香川大学大学院医学系研究科

医学専攻

RAHMAN SM KHALEDUR

BBA - Molecular and Cell Biology of Lipids 1867 (2022) 159222

Contents lists available at ScienceDirect

BBA - Molecular and Cell Biology of Lipids

journal homepage: www.elsevier.com/locate/bbalip

Formation of *N*-acyl-phosphatidylethanolamines by cytosolic phospholipase $A_2\varepsilon$ in an ex vivo murine model of brain ischemia

S.M. Khaledur Rahman [a,1], Zahir Hussain [a,b,1], Katsuya Morito [c], Naoko Takahashi [d], Mohammad Mamun Sikder [a], Tamotsu Tanaka [e], Ken-ichi Ohta [f], Masaki Ueno [g], Hiroo Takahashi [h], Tohru Yamamoto [h], Makoto Murakami [i], Toru Uyama [a,*], Natsuo Ueda [a,*]

[a] *Department of Biochemistry, Kagawa University School of Medicine, Kagawa, Japan*
[b] *Department of Pathology, McGowan Institute for Regenerative Medicine, University of Pittsburgh School of Medicine, Pittsburgh, PA, USA*
[c] *Department of Environmental Biochemistry, Division of Biological Sciences, Kyoto Pharmaceutical University, Kyoto, Japan*
[d] *Graduate School of Biomedical Sciences, Tokushima University, Tokushima, Japan*
[e] *Graduate School of Technology, Industrial and Social Sciences, Tokushima University, Tokushima, Japan*
[f] *Department of Anatomy and Neurobiology, Kagawa University School of Medicine, Kagawa, Japan*
[g] *Department of Pathology and Host Defense, Kagawa University School of Medicine, Kagawa, Japan*
[h] *Department of Molecular Neurobiology, Kagawa University School of Medicine, Kagawa, Japan*
[i] *Laboratory of Microenvironmental and Metabolic Health Science, Center for Disease Biology and Integrative Medicine, Faculty of Medicine, The University of Tokyo, Tokyo, Japan*

ARTICLE INFO

Keywords:
N-acylethanolamine
N-acyl-phosphatidylethanolamine
N-acyltransferase
Brain ischemia
Endocannabinoid
Phospholipase A_2

ABSTRACT

N-Acyl-phosphatidylethanolamines (NAPEs), a minor class of membrane glycerophospholipids, accumulate along with their bioactive metabolites, *N*-acylethanolamines (NAEs) during ischemia. NAPEs can be formed through *N*-acylation of phosphatidylethanolamine by cytosolic phospholipase $A_2\varepsilon$ ($cPLA_2\varepsilon$, also known as PLA2G4E) or members of the phospholipase A and acyltransferase (PLAAT) family. However, the enzyme responsible for the NAPE production in brain ischemia has not yet been clarified. Here, we investigated a possible role of $cPLA_2\varepsilon$ using $cPLA_2\varepsilon$-deficient (*Pla2g4e*$^{-/-}$) mice. As analyzed with brain homogenates of wild-type mice, the age dependency of Ca^{2+}-dependent NAPE-forming activity showed a bell-shape pattern being the highest at the first week of postnatal life, and the activity was completely abolished in *Pla2g4e*$^{-/-}$ mice. However, liquid chromatography-tandem mass spectrometry revealed that the NAPE levels of normal brain were similar between wild-type and *Pla2g4e*$^{-/-}$ mice. In contrast, post-mortal accumulations of NAPEs and most species of NAEs were only observed in decapitated brains of wild-type mice. These results suggested that $cPLA_2\varepsilon$ is responsible for Ca^{2+}-dependent formation of NAPEs in the brain as well as the accumulation of NAPEs and NAEs during ischemia, while other enzyme(s) appeared to be involved in the maintenance of basal NAPE levels.

1. Introduction

N-Acyl-phosphatidylethanolamine (NAPE), first isolated from the infarcted myocardium of dogs [1], is a membrane phospholipid traceably found in animals and plants under normal physiological conditions [2]. Its unique triacylated structure stabilizes cell membrane and serves as the precursor of lipid mediator *N*-acylethanolamines (NAEs) [3], including anti-inflammatory palmitoylethanolamide (PEA) [4],

Abbreviations: NAE, *N*-acylethanolamine; NAPE, *N*-acyl-phosphatidylethanolamine; AEA, arachidonoylethanolamide; CRISPR/Cas9, clustered regularly interspaced short palindromic repeats/CRISPR-associated protein 9; $cPLA_2\varepsilon$, cytosolic phospholipase $A_2\varepsilon$; DHEA, docosahexaenoylethanolamide; DTT, dithiothreitol; FAAH, fatty acid amide hydrolase; GAPDH, glyceraldehyde 3-phosphate dehydrogenase; LC-MS/MS, liquid chromatography-tandem mass spectrometry; MPC, medial prefrontal cortex; NAPE-PLD, NAPE-hydrolyzing phospholipase D; OEA, oleoylethanolamide; PC, phosphatidylcholine; PCR, polymerase chain reaction; PE, phosphatidylethanolamine; PEA, palmitoylethanolamide; PLAAT, phospholipase A and acyltransferase; PLA2G4E, phospholipase A_2 Group IVE; PS, phosphatidylserine; PSC, primary somatosensory cortex; qPCR, quantitative PCR; TLC, thin-layer chromatography; WT, wild-type.

* Corresponding authors at: Department of Biochemistry, Kagawa University School of Medicine, 1750-1 Ikenobe, Miki, Kagawa 761-0793, Japan.
E-mail addresses: uyama.toru@kagawa-u.ac.jp (T. Uyama), ueda.natsuo@kagawa-u.ac.jp (N. Ueda).

[1] These authors contributed equally to this work.

https://doi.org/10.1016/j.bbalip.2022.159222
Received 27 June 2022; Received in revised form 8 August 2022; Accepted 15 August 2022
Available online 19 August 2022

anorectic oleoylethanolamide (OEA) [5], the endocannabinoid arachidonoylethanolamide (AEA, anandamide) [6] and docosahexaenoylethanolamide (DHEA, synaptamide) which promotes neurogenesis, neuritogenesis and synaptogenesis [7]. In mammals, NAPE is enzymatically synthesized by *N*-acyltransferase which transfers an acyl chain of glycerophospholipid such as phosphatidylcholine (PC) to the amino group of phosphatidylethanolamine (PE) (Fig. 1) [8]. This NAPE is next hydrolyzed to NAE directly by NAPE-hydrolyzing phospholipase D (NAPE-PLD) [9] or through multi-step pathways via the formation of lysoNAPE [10] (Fig. 1). So far, it has been revealed that *N*-acyltransferases are classified into two groups on the basis of Ca^{2+}-dependency. The phospholipase A and acyltransferase (PLAAT) family, consisting of five members (PLAAT-1–5) in humans and three in rodents (PLAAT-1, -3, and -5), function as Ca^{2+}-independent *N*-acyltransferase [11], while the ε isoform of cytosolic phospholipase A_2 (cPLA$_2$ε), also referred to as phospholipase A_2 Group IVE (PLA2G4E), was identified as Ca^{2+}-dependent *N*-acyltransferase [12]. We also confirmed that the purified recombinant cPLA$_2$εs of mice and humans absolutely require Ca^{2+} for their *N*-acyltransferase activities [13,14]. Very recently, a *cPLA$_2$ε* gene-disrupted study showed its protective role against skin inflammation in an imiquimod-induced psoriatic mouse model by producing NAPEs to serve as the precursors of anti-inflammatory NAEs [15].

Brain contains a relatively high level of NAPE among various mouse and rat tissues [16]. In accordance with this finding, mRNA of *cPLA$_2$ε* is abundantly expressed in mouse brain [12]. Age-dependent change of brain *N*-acyltransferase activity has also been noted with higher activity in neonatal brain than that of adult counterparts [17,18]. In agreement with this finding, the expression level of *cPLA$_2$ε* was also higher in neonatal brain [12]. These results suggested that cPLA$_2$ε is the principal *N*-acyltransferase responsible for NAPE generation in brain. However, mouse brain also expresses PLAAT family members; the expression level of PLAAT-1 was relatively high in brain [19], and PLAAT-3 and -5 showed moderate and low expressions, respectively [20,21]. It was likely that other enzyme(s) also function as *N*-acyltransferase. Therefore, it has not yet been elucidated how much cPLA$_2$ε is responsible for the formation of NAPEs in the brain in vivo.

In the present study, we analyzed the brain of *cPLA$_2$ε* gene-disrupted (*Pla2g4e$^{-/-}$*) mice and showed that cPLA$_2$ε is responsible for the brain Ca^{2+}-dependent *N*-acyltransferase activity. Furthermore, we focused on the post-decapitative brain ischemic model, in which NAPEs and NAEs were reported to remarkably accumulate [17,18,22,23]. Since cPLA$_2$ε was suggested to be activated by the increase in intracellular Ca^{2+} concentration triggered by cell damage [14], we expected that *Pla2g4e$^{-/-}$* mice are useful to elucidate the contribution of cPLA$_2$ε to the post-mortal accumulation of NAPEs and NAEs. Our results demonstrated for the first time the central role of cPLA$_2$ε in this ischemic model and also suggested the involvement of other enzyme(s) in the maintenance of basal levels of NAPEs, namely, the NAPE levels in the non-damaged brain tissue.

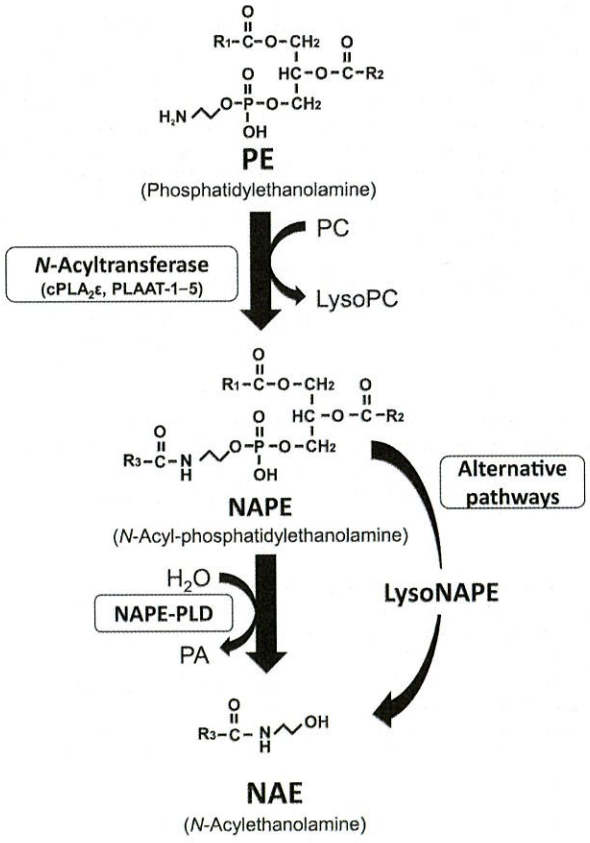

Fig. 1. NAE-biosynthetic pathway.
The outline of NAE biosynthetic pathway in mammals is shown. PA, phosphatidic acid.

2. Materials and methods

2.1. Materials

1,2-[1′-^{14}C]Dipalmitoyl-PC was purchased from PerkinElmer Life Science (Boston, MA, USA). 1,2-Dipalmitoyl-PC and 1,2-dioleoyl-PE were from Sigma-Aldrich (St. Louis, MO, USA). 1,2-Dioleoyl-phosphatidylserine (PS) was from Avanti Polar Lipids (Alabaster, AL, USA). Nonidet P-40 was from Nacalai Tesque (Kyoto, Japan). Dithiothreitol (DTT), 3(2)-*t*-butyl-4-hydroxyanisole and isoflurane were from Wako Pure Chemical (Osaka, Japan). Protein assay dye reagent concentrate was from Bio-Rad (Hercules, CA, USA). Precoated silica gel 60 F_{254} aluminum sheets (20 × 20 cm, 0.2 mm thick) for thin-layer chromatography (TLC) were from Merck (Darmstadt, Germany). Wild-type (WT) C57BL/6 mice were from Japan SLC Inc. (Shizuoka, Japan). Quick Taq HS DyeMix was from TOYOBO (Osaka, Japan). PrimeScript RT reagent kit and SYBR Premix Ex Taq II were from Takara Bio (Ohtsu, Japan). TRIzol was from Thermo Fisher Scientific (Waltham, MA, USA).

2.2. Generation of *Pla2g4e$^{-/-}$* mice

Pla2g4e$^{-/-}$ mice were generated as reported by Liang et al. [15]. Briefly, exon-11 of *Pla2g4e* gene underwent a deletion of 13 base-pairs by the clustered regularly interspaced short palindromic repeats/CRISPR-associated protein 9 (CRISPR/Cas9) system. This deletion caused a frameshift mutation making a new stop codon just after the 402nd amino acid resulting in a truncated protein. This truncated protein did not contain Ser-420, which was previously reported to be the catalytic nucleophile [12]. The obtained *Pla2g4e$^{+/-}$* mice were backcrossed to C57BL/6 genetic background and were intercrossed to WT and *Pla2g4e$^{-/-}$* mice. *Pla2g4e$^{-/-}$* mice were born at the expected Mendelian frequency, viable, and healthy [15].

2.3. PCR-based genotyping

The genomic DNA obtained from mouse tails was subjected to conventional PCR. The primers used were 5′-CAAGGTCTATGGTCTCCTTG-3′ (forward for WT), 5′-TGGCACAAGGTCTATGGCCA-3′ (forward for *Pla2g4e$^{-/-}$*), and 5′-ATGTATACAGCAGCTCTGTGC-3′ (reverse for both WT and *Pla2g4e$^{-/-}$*). PCR amplification was performed with Quick Taq HS DyeMix at a denaturing temperature of 94 °C for 30 s, followed by annealing at 60 °C for 30 s and extension at 68 °C for 30 s (35 cycles). The WT-specific primer set and the *Pla2g4e$^{-/-}$*-specific primer set produced 254 bp allele and 246 bp allele, respectively.

2.4. Animal experiments

The protocol of this study was approved by the Animal Care and Use Committee for Kagawa University (approved numbers: 2021-21619). Mice were maintained in a temperature-controlled room (22 ± 2 °C) with 12 h of light/dark cycle (lights on from 0600 to 1800) and were given food and water ad libitum.

Pregnant mice of WT or *Pla2g4e*$^{-/-}$ were allowed to give birth spontaneously and the day of birth was designated as postnatal day 0 (P0). Mice were anesthetized with isoflurane and sacrificed by cervical dislocation. Some pregnant mice were sacrificed before term to collect embryos at day 14 (E14) and 17 (E17). Whole brain tissues from mice were immediately frozen in liquid N_2 and stored at −80 °C until use.

2.5. Region-specific sampling of brain tissue

WT male pups at P7 age ($n = 3$) were anesthetized and sacrificed by decapitation. Whole brains were removed from the skulls and sectioned in the coronal plane to yield 1-mm-thick slices using a Brain Matrix device (Roboz Surgical Instrument, MD, USA). Various brain regions were dissected from these slices. Samples were immediately frozen in liquid N_2 and stored at −80 °C until use. The membrane fractions were then prepared from the brain homogenates as described below and used for *N*-acyltransferase assay.

2.6. Real-time quantitative PCR (qPCR)

Total RNAs were collected from mouse brain tissues at the age of E14, E17, P0, P7, P14, P21 and P28 ($n = 3$ for each age) by TRIzol, and cDNAs were synthesized with PrimeScript RT reagent kit. qPCR was performed with an Applied Biosystems ViiA7 Real-Time PCR System (Thermo Fisher Scientific, Carlsbad, CA) using SYBR Premix Ex Taq II. The primers used for *cPLA$_2\varepsilon$* and glyceraldehyde 3-phosphate dehydrogenase (*GAPDH*) (an endogenous control) are shown in Table 1. The PCR conditions were as follows: denaturation at 95 °C for 5 s and annealing/extension at 60 °C for 30 s (40 cycles). The cDNAs of WT P7 mouse brain were serially diluted (1:2 for *cPLA$_2\varepsilon$* and 1:4 for *GAPDH*) and used to draw standard curves by plotting the threshold cycles versus $\log_{10}$ of arbitrary relative initial quantities of cDNAs.

2.7. Enzyme assay

After sacrifice, the brain tissues of WT and *Pla2g4e*$^{-/-}$ mouse (mixed sexes) at the age of E14, E17, P0, P7, P14, P21 and P28 ($n = 3$ for each age) were removed and homogenized in 5 volumes (*v/w*) of 20 mM Tris-HCl (pH 7.4) containing 0.32 M sucrose using a Polytron homogenizer. The cell-free extracts were first centrifuged at 800 ×*g* for 15 min, and the supernatant (designated as homogenates) was further centrifuged at 105,000 ×*g* for 55 min. The obtained pellet was suspended in 20 mM Tris-HCl (pH 7.4) containing 0.32 M sucrose and used as the membrane fraction. For *N*-acyltransferase assay, 50 μg protein of membrane fraction was incubated with 25 μM 1,2-[^{14}C]dipalmitoyl-PC (90,000 cpm) and 100 μM 1,2-dioleoyl-PE in 100 μL of 100 mM Tris-HCl (pH 8.2) containing 100 μM dioleoyl-PS, 2 mM DTT, 0.05 % Nonidet P-40 and either of 5 mM $CaCl_2$ or 5 mM EGTA at 37 °C for 60 min. The reaction was terminated by the addition of 320 μL of a mixture of chloroform and methanol (2:1, *v/v*) containing 5 mM 3(2)-*t*-butyl-4-hydroxyanisole. After centrifugation, 100 μL of the organic phase was spotted on a silica gel thin-layer plate (10 cm height) with a calibrated capillary glass pipet connected to a rubber aspirator tube (Drummond Scientific Co., Broomall, PA) and was dried under the airflow of a hair dryer. The plate was next developed at 4 °C for 25 min in a mixture of chloroform/methanol/28 % ammonium hydroxide (80:20:2, *v/v*) resulting in the separation of the produced *N*-[^{14}C]palmitoyl-PE from other radioactive compounds. The proper identification of the product was confirmed by comigration with the authentic standard of *N*-[^{14}C]palmitoyl-PE on the same TLC plate in three different solvents: chloroform/methanol/28 % ammonium hydroxide (80:20:2, *v/v*), chloroform/methanol/water (65:25:4, *v/v*), and chloroform/methanol/acetic acid (9:1:1, *v/v*). For this purpose, *N*-[^{14}C]palmitoyl-PE was synthesized from [1-^{14}C]palmitic acid and 1,2-dioleoyl-PE according to the method of Tsuboi et al. [10]. The distribution of radioactivity on the plate was visualized and quantified using an image reader FLA-7000 (Fujifilm, Tokyo, Japan). The *N*-acyltransferase activity was calculated by quantifying *N*-[^{14}C]palmitoyl-PE.

2.8. Post-decapitative ischemia

P7 WT and *Pla2g4e*$^{-/-}$ mice of mixed sexes were anesthetized and sacrificed by decapitation. The heads were wrapped in aluminum foil and incubated at 37 °C for 6 h, as described previously [18]. As controls, the removed heads were immediately frozen in liquid N_2. These brain samples were stored at −80 °C until use.

2.9. Analysis of NAPEs and NAEs by liquid chromatography-tandem mass spectrometry (LC-MS/MS)

The brains were suspended in 3.8 mL of a mixture of chloroform/methanol/2.0 % KCl (1:2:0.8, *v/v*) on ice followed by homogenization using a TissueRuptor II (Qiagen, Hilden, Germany) for several minutes. After adding internal standards (Table 2), the homogenates were sonicated for 10 s in an ultrasonic bath sonicator and then centrifuged at 1100 ×*g* for 5 min. The supernatant was withdrawn, and the resulting pellet was mixed with 1.9 mL of chloroform/methanol/2.0 % KCl (1:2:0.8, *v/v*) followed by another centrifugation. Supernatants were combined and mixed with 1.5 mL each of chloroform and water, followed by centrifugation at 1100 ×*g* for 5 min. The resulting lower layer was transferred to another glass tube. The remaining upper layer was

Table 2
Conditions for LC-MS/MS.

	NAPE	NAE
Internal standard	16:0/16:0/N17:0-NAPE (1 nmol)	$d_4$16:0 NAE (0.1 nmol)
Selected ions		
Q1	$[M - H]^-$	$[M + H]^+$
Q3*	$[R_2COO]^-$	*m/z* 62
Column**	a	b
Solvent***	A	B

* $[R_2COO]^-$, acyl chain released from *sn*-2 position; *m/z* 62, ethanolamine ion.
** a, Imtakt Unison UK-amino (100 × 2 mm, 3 μm); b, Supelco Ascentis Express C18 reverse-phase (150 × 2.1 mm, 2.7 μm).
*** A, acetonitrile/methanol (95:5, *v/v*) containing 0.1 % triethylamine; B, methanol/water (95:5, *v/v*) containing 5 mM ammonium formate.

Table 1
Primers used for qPCR.

cDNA (accession number)	Direction	Sequence	Location of nucleotides
Pla2g4e	Forward	5′-AAACACCTGAACCTGCTGGACACTGCG-3′	2532–2558
(NM_177845)	Reverse	5′-TCTTCTGCTCGGTACAGTACTCACAGG-3′	2694–2668
GAPDH	Forward	5′-AACTCCCACTCTTCCACCTTCGATG-3′	1099–1123
(NM_008084)	Reverse	5′-CCTGTTGCTGTAGCCGTATTCATTG-3′	1203–1179

mixed with 3 mL of chloroform/methanol (17:3, *v/v*) and centrifuged. The lower layer was combined with the former one. After evaporation, one-third of lipids recovered from the combined lower layers were dissolved in 0.8 mL of methanol. The lipid solution was filtered through a non-polar filter (Chromatodisc 4N, 0.2 μm, Kurabo, Osaka, Japan). The filtrate was dissolved in 1.5 mL of a mixture of methanol/water (95:5, *v/v*) containing 5 mM ammonium formate for LC-MS/MS. In the case of NAPE analysis, lipids were dissolved in the solvent without ammonium formate. LC-MS/MS was performed using a quadrupole-linear ion trap hybrid mass spectrometer, 4000 Q TRAP (Applied Biosystems/MDS Sciex, Concord, Ontario, Canada) with an Agilent 1100 liquid chromatograph (Agilent Technologies, Wilmington DE, USA) and HTSPAL autosampler (CTC Analytics AC, Zwingen, Switzerland), as described previously [10,24,25]. The internal standards, selected ions, and LC conditions for LC-MS/MS are summarized in Table 2. The amounts of lipid molecules were determined from ratios of peak areas of objective lipid molecules to those of their corresponding internal standards and were shown as nmol/g tissue. Although the ionizing efficiency of lipid molecules in electrospray ionization varies depending on the chain-length and number of double bonds in the molecule, the differences in the ionizing efficiency were not taken into consideration. The amounts of alkenylacyl-type NAPE were corrected by using correction factors as described previously [10,26]. Statistical analyses were performed by one-way ANOVA with post hoc Tukey's test.

2.10. Histological analysis of brain

Whole brains were collected from P7 and P30 mice under anesthesia and fixed with 4 % paraformaldehyde in PBS. The brains were embedded in paraffin and sectioned sagittally at a thickness of 4 μm. The sections were stained with hematoxylin and eosin, followed by histological examination.

3. Results

3.1. Age-dependent expression of cPLA$_2\varepsilon$ in mouse brain

Since Ca^{2+}-dependent *N*-acyltransferase activity changes age-dependently in brain [17,18], we first quantified the mRNAs of *cPLA$_2\varepsilon$* at various ages (E14–P28) from WT mouse brain by qPCR (Fig. 2A).

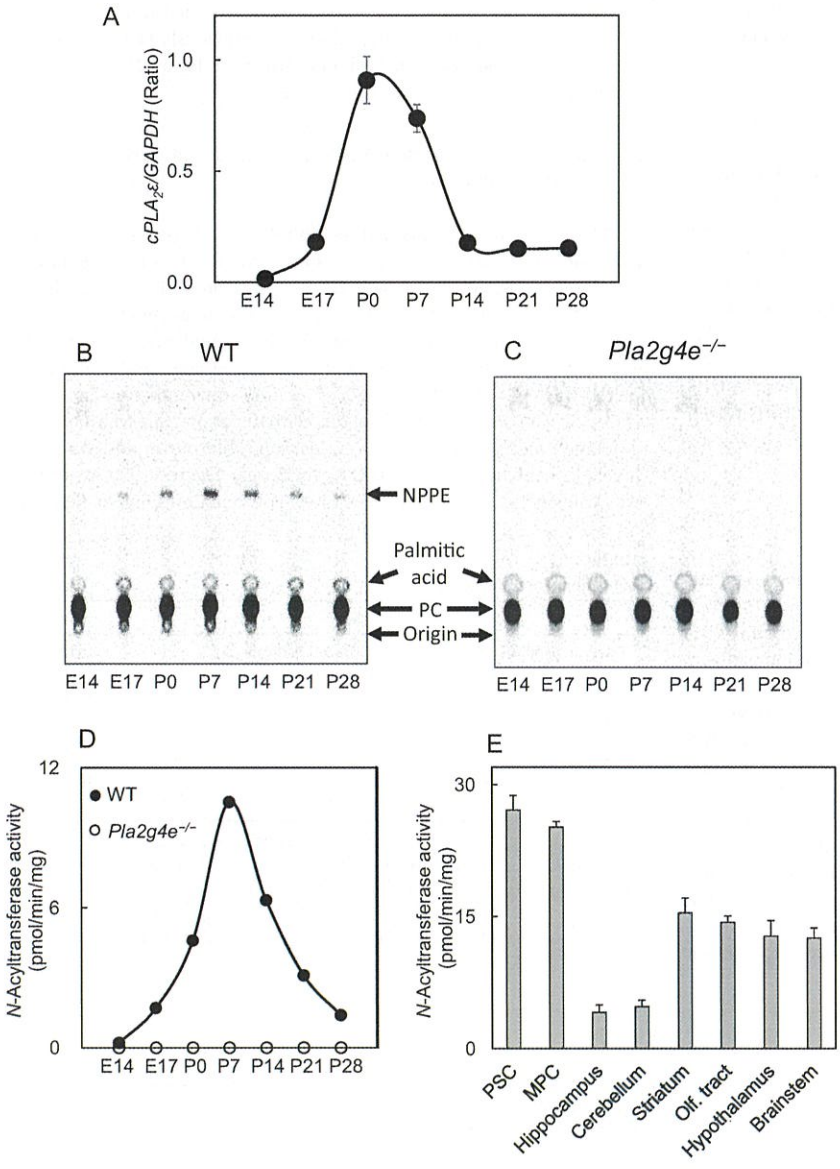

Fig. 2. Age-dependent changes of cPLA$_2\varepsilon$ expression and *N*-acyltransferase activity in mouse brain.
The mRNA levels of *cPLA$_2\varepsilon$* in WT mouse brain at the indicated ages were measured by qPCR. The expression levels of these mRNAs were normalized to those of *GAPDH* and the ratios were shown (mean values ± SD, $n = 3$) (A). The membrane fractions (50 μg of protein) of WT and *Pla2g4e*$^{-/-}$ mouse brains at the indicated ages were assayed for *N*-acyltransferase activity. The resultant radioactive products were separated by TLC for WT (B) and *Pla2g4e*$^{-/-}$ (C), and *N*-acyltransferase activities were calculated by quantifying the produced *N*-[^{14}C]palmitoyl-PE (NPPE) (mean values ± SD, $n = 4$) (D). The membrane fractions (25 μg of protein) of cortex (PSC and MPC), hippocampus, cerebellum, striatum, olfactory tract, hypothalamus, and brainstem in P7 WT mouse brain were also assayed for *N*-acyltransferase activity (mean values ± SD, n = 3) (E).

When normalized to *GAPDH* levels, *cPLA$_2\varepsilon$* mRNA levels started to increase at E14 being the highest at P0 and then slowly went downhill until reaching plateau at P14. The *cPLA$_2\varepsilon$* expression was estimated to be around 13-fold higher at P0 than E14, but about 6-times lower at the plateau level (P14–P28) than P0.

3.2. Age-dependent N-acyltransferase activity in mouse brain

We next examined Ca^{2+}-dependent *N*-acyltransferase activity in the brains of WT and *Pla2g4e*$^{-/-}$ mice at the same age points (Fig. 2B–D). For this purpose, we used membrane fractions of brain homogenates since cPLA$_2\varepsilon$ was reported to be rich in membrane [27]. The activity of WT was first detectable at E17 and continued to increase until P7, followed by a sharp decline towards the older age points. The highest activity detected at P7 was 10.5 pmol/min/mg, which was around 7-fold higher than the lowest detectable activity found at either E17 or P28. The activity did not change significantly after P28 and remained almost same until P70 (data not shown). Therefore, we used P28 or P30 mice rather than adult mice hereafter. When $CaCl_2$ was replaced with EGTA as Ca^{2+} chelator, the activity could not be detected at all (data not shown). In contrast, the activity was not detectable in *Pla2g4e*$^{-/-}$ mouse brain at any of the tested age points even in the presence of Ca^{2+} (Fig. 2C and D). These results strongly suggested that cPLA$_2\varepsilon$ is responsible for the Ca^{2+}-dependent formation of NAPEs by the membrane fraction of mouse brain where its activity remarkably changed in the early stages of life.

3.3. Distribution of cPLA$_2\varepsilon$ activity in mouse brain

In order to find the spatial distribution of cPLA$_2\varepsilon$ in the brain, membrane fractions of several regions of the brain prepared from WT mice at P7 were analyzed for the Ca^{2+}-dependent *N*-acyltransferase activity (Fig. 2E). The activity was found to be the highest in the cortical regions (27.1 and 25.2 pmol/min/mg in primary somatosensory cortex (PSC) and medial prefrontal cortex (MPC), respectively), the lowest in hippocampus (4.1) and cerebellum (4.7), and intermediate in striatum (15.4), olfactory tract (14.3), hypothalamus (12.8) and brainstem (12.6). These activities were not detected in the identical brain regions of *Pla2g4e*$^{-/-}$ mouse at P7 (data not shown), suggesting the central role of cPLA$_2\varepsilon$ in the NAPE production in various brain regions. Histological studies on the brains of WT and *Pla2g4e*$^{-/-}$ mice at P7 and P30 revealed that there was no clear morphological difference between the two groups (Supplementary Figs. 1 and 2).

3.4. cPLA$_2\varepsilon$-independent mechanism is responsible for maintenance of basal NAPE levels

We next analyzed endogenous NAPE levels of whole brains from WT and *Pla2g4e*$^{-/-}$ mice by LC-MS/MS. Considering the age-dependent change of *cPLA$_2\varepsilon$* expression levels, we used mice at P7 and P30. The whole brains were removed and immediately frozen in liquid nitrogen. Total lipids were then extracted from the whole brains and analyzed for total levels of diacyl- and alkenylacyl-NAPEs (Fig. 3). Surprisingly, both types of NAPEs could be detected even in *Pla2g4e*$^{-/-}$ mice, and their levels were not significantly different from those of WT mice at the corresponding ages. Moreover, throughout the transition from P7 towards P30, total NAPE levels increased by >4-fold in WT and *Pla2g4e*$^{-/-}$ mouse brain, which were unexpected results since the *cPLA$_2\varepsilon$* expression level and activity at P7 were much higher than those at P28 as shown in Fig. 2A and D, respectively. These results suggested that other enzyme(s) are responsible to maintain the basal brain levels, namely, NAPE levels in non-damaged brain tissue.

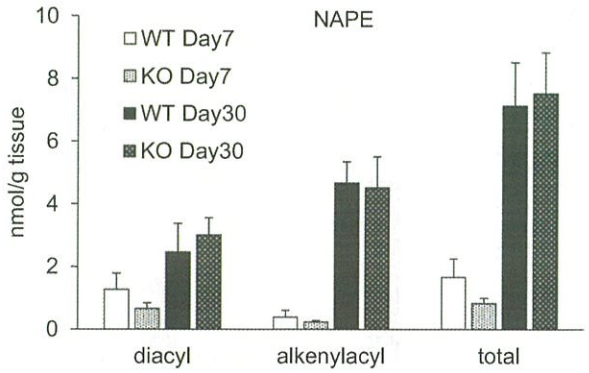

Fig. 3. Brain levels of total NAPEs in WT and *Pla2g4e*$^{-/-}$ mice.
Lipids were extracted from the brains of WT and *Pla2g4e*$^{-/-}$ (KO) mice at the indicated ages and analyzed for total diacyl-type and alkenylacyl-type of NAPEs by LC-MS/MS (mean values ± SD, $n = 4$). Each molecular species of diacyl-type and alkenylacyl-type of NAPEs was measured, and their summations were shown, respectively.

3.5. cPLA$_2\varepsilon$ is responsible for post-decapitative accumulation of NAPEs in brain

In order to investigate the role of cPLA$_2\varepsilon$ in brain ischemia, we next used decapitated brains of WT and *Pla2g4e*$^{-/-}$ mouse at P7, which were incubated at 37 °C for 6 h after decapitation. As controls, we used the brains frozen immediately after decapitation (designated as 0 h). We then analyzed NAPEs and NAEs by LC-MS/MS.

As compared for the total NAPE levels, both diacyl- and alkenylacyl-type of NAPEs showed similar levels between WT and *Pla2g4e*$^{-/-}$ mouse brain at 0 h (Fig. 4A and Supplementary Table 1), which agreed with the results of Fig. 3. As reported previously [17,18], 6 h-incubation of WT mouse brain remarkably increased the endogenous levels of diacyl- and alkenylacyl-type of NAPEs (20.5-fold and 8.5-fold, respectively). In contrast, *Pla2g4e*$^{-/-}$ mouse brain just maintained the basal level of NAPEs.

As for different acyl species of NAPEs, total 20 diacyl-type (Fig. 5A and Supplementary Table 2) and 13 alkenylacyl-type of NAPEs (Fig. 5B and Supplementary Table 3) were detected as major species, where 18:1 mostly occupied the *sn*-2 position as reported previously for diacyl-type NAPE in brain tissue [10,12]. All these species of NAPEs increased significantly in WT mice at 6 h in comparison to 0 h, while *Pla2g4e*$^{-/-}$ mice showed almost no changes, suggesting that cPLA$_2\varepsilon$ is mainly responsible for the post-mortal generation of all these species of NAPEs in the brain.

3.6. cPLA$_2\varepsilon$ is responsible for post-decapitative accumulation of most species of NAEs in brain

WT mouse brain also produced 219-fold more NAEs at 6 h, but *Pla2g4e*$^{-/-}$ mouse brain produced only 8.7-fold more NAEs (Fig. 4B and Supplementary Table 1). These results strongly suggested that the NAPEs produced by cPLA$_2\varepsilon$ during brain ischemia served as precursors of NAEs.

As for different acyl species of NAEs, 18 types of NAEs, including PEA (16:0-NAE), stearoylethanolamide (18:0-NAE) and OEA (18:1-NAE), were detected (Fig. 6 and Supplementary Table 4). Among them almost all the species increased in WT-6 h in comparison with WT-0 h (392, 208 and 104 fold for 16:0-, 18:0- and 18:1-NAE, respectively). In contrast, the *Pla2g4e*$^{-/-}$ mouse counterparts produced the same or slightly higher levels of NAEs in most cases (Supplementary Table 4). However, AEA (20:4-NAE) was found to be significantly increased in both WT and *Pla2g4e*$^{-/-}$ mice at 6 h (64- and 29-fold, respectively). DHEA (22:6-NAE) also increased in both WT and *Pla2g4e*$^{-/-}$ mice (10- and 4.3-fold,

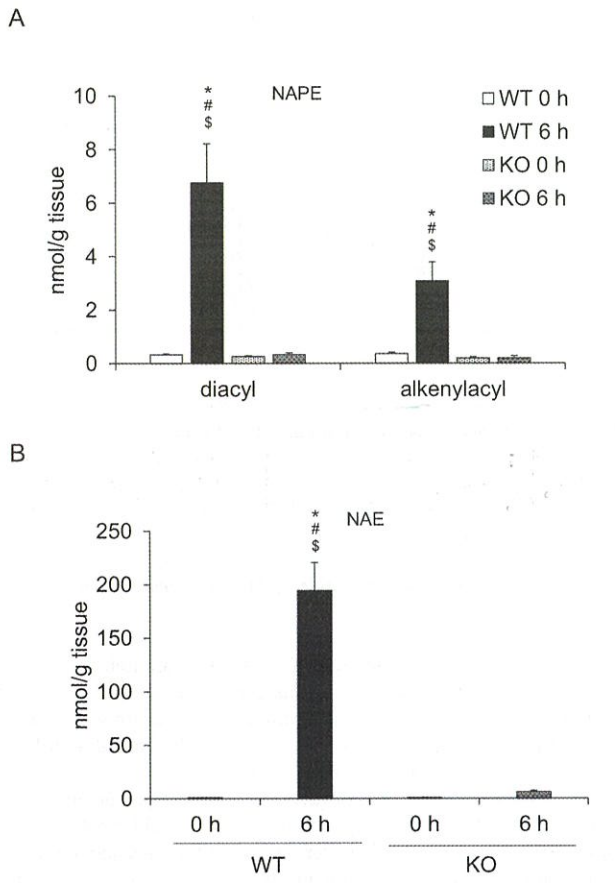

Fig. 4. Post-decapitative accumulation of total NAPEs and NAEs in the brains of WT and *Pla2g4e*$^{-/-}$ mice.
Lipids were extracted from the decapitated P7 WT and *Pla2g4e*$^{-/-}$ (KO) mouse brains at 0 h or after incubation at 37 °C for 6 h and analyzed for total NAPEs (A) and NAEs (B) by LC-MS/MS. Each molecular species of NAPE and NAE was originally measured in the experiments of Figs. 5 and 6, respectively, and their summations were shown in this figure. Results are shown as mean values ± SD ($n = 4$). $^{*}P < 0.05$ versus WT 0 h, $^{\#}P < 0.05$ versus KO 0 h, $^{\$}P < 0.05$ versus KO 6 h, respectively. Statistical analyses were performed by one-way ANOVA with post hoc Tukey's test.

respectively). These results suggested that the increase of NAE levels in the post-decapitative brain is principally attributed to the stimulation of cPLA$_2\varepsilon$, but other mechanism(s), which bypass NAPE, also appeared to exist especially in the generation of these two polyunsaturated NAEs (AEA and DHEA).

4. Discussion

Under normal physiological conditions, mammals produce very low levels of NAPEs (~0.01 % of total phospholipids) [16]. However, certain pathologic conditions such as ischemia cause rapid accumulation of NAPEs and their more important downstream metabolites, NAEs [2,23,28,29]. This on-demand nature of production implies that the enzymes responsible for their biosynthetic and degradative pathways play the major regulatory roles [11,30]. So far, NAPE-formation is considered as the rate-limiting step triggering the whole cascade of NAE-biosynthesizing system and is catalyzed by two types of *N*-acyltransferase distinguished by Ca^{2+}-dependency [11]. Ca^{2+}-dependent cPLA$_2\varepsilon$ (also referred to as PLA2G4E) and Ca^{2+}-independent PLAAT family members are the first line putative candidate enzymes for the formation of NAPEs as is evident from their previous in vitro characterizations [11]. Due to the Ca^{2+}-dependence, cPLA$_2\varepsilon$ was proposed to be responsible for the large pool of NAPEs and NAEs accumulated during ischemia while Ca^{2+}-independent PLAAT family members were suggested to maintain their basal levels [14]. However, there was no direct evidence to show that cPLA$_2\varepsilon$ is required to generate NAPE in vivo as well as its relevance with ischemia. In order to clarify this question, we have used *Pla2g4e*$^{-/-}$ mice in the present study and measured NAPE-forming activity as well as endogenous levels of NAPEs and NAEs in the whole brain from these animals.

Ca^{2+}-dependent NAPE formation was previously reported to be age-dependently altered in rat brains [17,18]. For example, post-decapitative accumulation of NAPE, presumed to be a Ca^{2+}-dependent process, was much higher in one-week-old rat brains than in one-month-old rat brains [18]. This was further supported by the observation of ~4-fold higher Ca^{2+}-dependent NAPE-forming activity of brain microsomes in one-week-old neonates than in one-month-old counterparts in the same study [18]. Due to the lack of genetic information, it was not possible to dig out more information about the enzyme responsible for this phenomenon for long time until Ogura et al. characterized recombinant cPLA$_2\varepsilon$ as a Ca^{2+}-dependent NAPE-producer in vitro [12]. They also showed that *cPLA$_2\varepsilon$*-expression and *N*-acyltransferase activity were ~4-fold higher in mouse postnatal 1-day-old brains than in 10-week-old counterparts. Consistent to these past findings, our present study showed that the highest expression of *cPLA$_2\varepsilon$* and the *N*-acyltransferase activity concur during the first week of mouse neonatal life. Importantly, in the present study the Ca^{2+}-dependent *N*-acyltransferase activity was completely abolished in *Pla2g4e*$^{-/-}$ mice at all the tested age points. Our LC-MS/MS analysis also revealed that post-decapitative accumulation of NAPEs in WT mouse brain at P7 was almost abolished in *Pla2g4e*$^{-/-}$ mouse brain at the same age. These results with *Pla2g4e*$^{-/-}$ mice strongly suggested that cPLA$_2\varepsilon$ is mostly responsible for the brain Ca^{2+}-dependent *N*-acyltransferase activity and post-decapitative accumulation of NAPEs at different ages. The Ca^{2+}-dependent *N*-acyltransferase activity derived from cPLA$_2\varepsilon$ was detected in all the brain regions with the highest in the cortical regions and the lowest in hippocampus and cerebellum (Fig. 2E). Although we did not measure endogenous NAPE/NAE levels in each region, it will be an interesting to see the correlation between regiospecific cPLA$_2\varepsilon$ expression and endogenous NAPE/NAE levels.

Since a low level of NAPE is detected in brain tissues under normal physiological conditions [16], where intracellular Ca^{2+} levels should be kept <0.1 μM at resting state [31], cPLA$_2\varepsilon$, requiring relatively high levels of Ca^{2+} for its activity with EC_{50} for Ca^{2+} being around 0.4 mM [14], might not be the only NAPE-forming enzyme. As Ca^{2+}-dependent NAPE-forming activity in vitro as well as *cPLA$_2\varepsilon$* expression showed drastic changes between the first week of neonatal life and around one-month-old mouse brains, we compared endogenous NAPE levels at P7 and P30. As expected, some NAPEs at basal levels remained in *Pla2g4e*$^{-/-}$ mice at both these ages and surprisingly, the basal levels at P30 were higher than those at P7. Because the higher levels of NAPEs at P30 than P7 did not agree with the age-dependent bell-shaped curve with the highest level of *cPLA$_2\varepsilon$* expression at P0–P7, these results suggested that other enzyme(s) are responsible to maintain the basal level of NAPEs in brain. The enzyme(s) responsible are probably independent of Ca^{2+}. However, it remains unclear if the Ca^{2+}-independent enzyme(s) are PLAAT family members (PLAAT-1, -3 or -5).

In our ischemic model, similar to the increased NAPE levels as discussed above, a large amount of NAEs, including quantitatively major PEA (~392-fold) and OEA (~104-fold) were produced in WT mouse brain. This suggests that cPLA$_2\varepsilon$ contributes to the generation of NAEs with various acyl species by generating their corresponding NAPEs. *N*-Acyl group of NAE is exclusively derived from *sn*-1 position of glycerophospholipids in the cPLA$_2\varepsilon$-catalyzed *N*-acylation [12] and various NAEs are almost equally released from their corresponding NAPEs by NAPE-PLD [9]. Since arachidonic and docosahexaenoic acids are dominant at *sn*-2 rather than *sn*-1 position of glycerophospholipids [32],

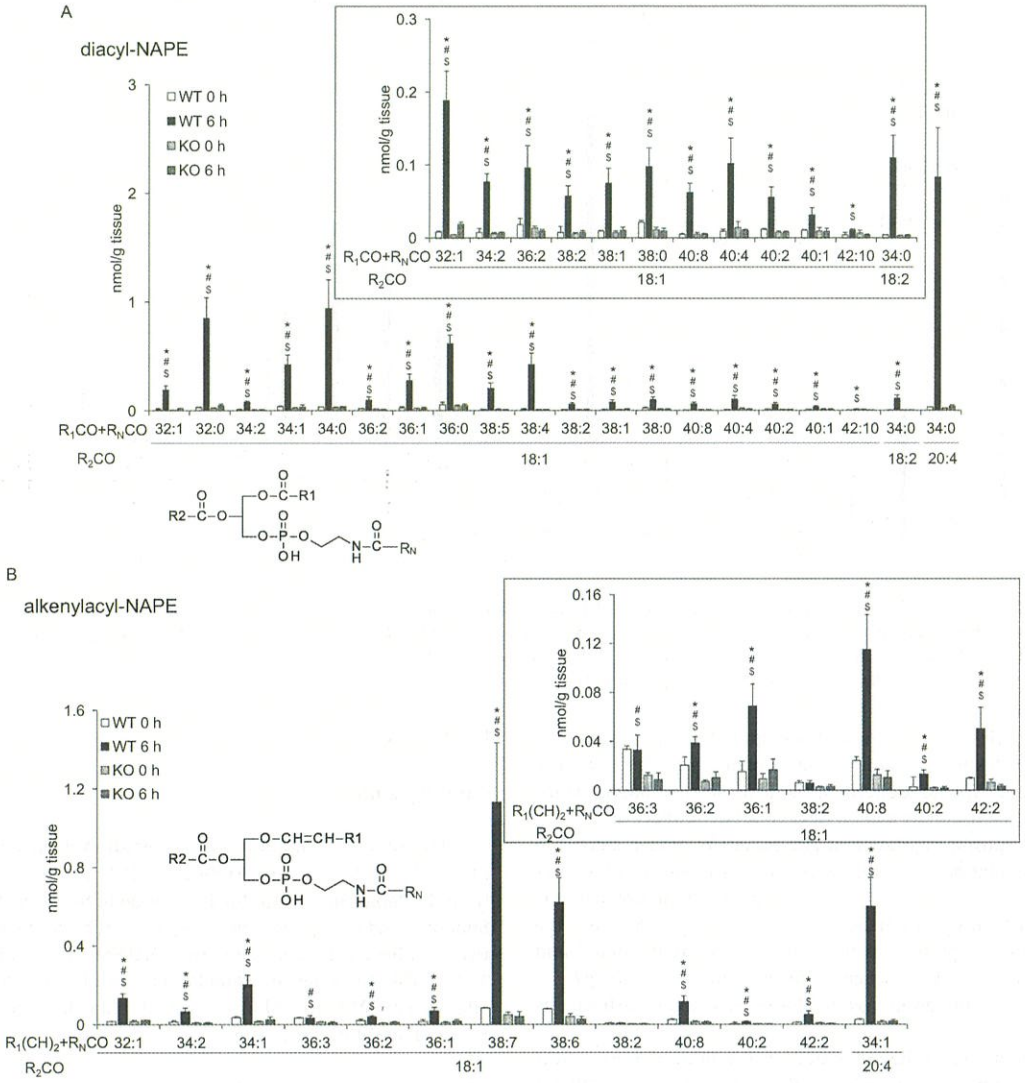

Fig. 5. Post-decapitative accumulation of various species of NAPEs in WT and *Pla2g4e*$^{-/-}$ mouse brains.
Lipids extracted from the of decapitated P7 WT and *Pla2g4e*$^{-/-}$ (KO) mouse brain at 0 h or after incubation at 37 °C for 6 h and were analyzed for diacyl-type (A) and alkenylacyl-type (B) of NAPEs by LC-MS/MS. Results are shown as mean values ± SD (n = 4). *$P < 0.05$ versus WT 0 h, $^{\#}P < 0.05$ versus KO 0 h, $^{\$}P < 0.05$ versus KO 6 h, respectively. Statistical analyses were performed by one-way ANOVA with post hoc Tukey's test.

AEA and DHEA are minor components among various NAPEs. AEA (~64-fold) and DHEA (~10-fold) were also increased in the brain after decapitation. This increase might be attributed to this route as expected by the presence of some NAPEs with four or more double bonds in R_N + R_1. However, the increases in these two NAEs were not fully correlated to the expression of *cPLA*$_2\varepsilon$ since their levels also increased in *Pla2g4e*$^{-/-}$ mice (~29- and ~4-fold, respectively), suggesting the presence of alternative pathways.

For example, Patel et al. previously reported that "post-mortal accumulation of brain anandamide is dependent upon fatty acid amide hydrolase (FAAH) activity", using *Faah*$^{-/-}$ mice [22]. FAAH is the major degrading enzyme for various NAEs including AEA (anandamide) [33]. On the other hand, in a dead cell, the increased intracellular Ca^{2+} may stimulate not only cPLA$_2\varepsilon$, but also other Ca^{2+}-dependent phospholipid-metabolizing enzymes such as cPLA$_2\alpha$, resulting in the release of large amounts of free fatty acid, including arachidonic and docosahexaenoic acids, from *sn*-2 position of glycerophospholipid [32] or through the pathway composed of phospholipase C, diacylglycerol lipase, and monoacylglycerol lipase [8]. In the reverse reaction of FAAH in vitro, NAEs can be synthesized from free fatty acids and ethanolamine, and arachidonic acid is a better substrate than palmitic acid [34]. Thus, anandamide and probably DHEA may be at least partly formed by the reverse reaction of FAAH in the brain of ischemic models. However, it remains unclear whether FAAH actually functions as 'NAE synthase' in vivo. Alternatively, the postmortem accumulation of AEA was proposed to occur by base-catalyzed aminolysis of arachidonate-containing glycerophospholipids [23].

Increased formation of NAPEs and NAEs during ischemic insult was previously suggested to be cytoprotective [16]. For example, NAPE is reported to stabilize cell membrane in vitro [3] and was recently suggested to play a protective role in 6-hydroxydopamine-induced neurodegeneration in *Napepld*$^{-/-}$ mice [35]. In addition, exogenous administration of NAEs such as PEA in rats [36] and OEA in mice [37] reduced infarct volume in the brain, suggesting that these NAEs exert neuroprotective effect. Involvement of peroxisome proliferator-activated receptor-α as a molecular target of PEA and OEA was suggested to be responsible for this protective effect [36]. Since we observed a high level of *cPLA*$_2\varepsilon$ expression and its potent NAPE-forming

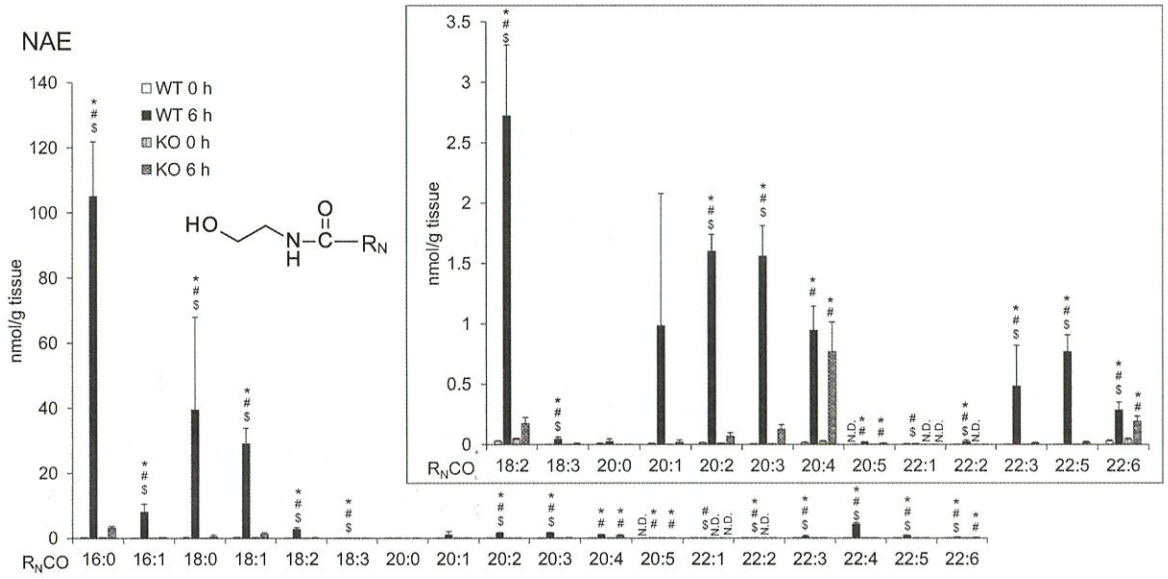

Fig. 6. Post-decapitative accumulation of various species of NAEs in WT and *Pla2g4e*$^{-/-}$ mouse brains.
Lipids extracted from the decapitated P7 WT and *Pla2g4e*$^{-/-}$ (KO) mouse brain at 0 h or after incubation at 37 °C for 6 h and were analyzed for various acyl species of NAEs by LC-MS/MS. Results are shown as mean values ± SD (n = 4). $^{*}P < 0.05$ versus WT 0 h, $^{\#}P < 0.05$ versus KO 0 h, $^{\$}P < 0.05$ versus KO 6 h, respectively. Statistical analyses were performed by one-way ANOVA with post hoc Tukey's test.

activity in brain during the first week of neonatal life, this enzyme may work as a standby NAPE generator for the neonates who are generally more susceptible to hypoxia-induced ischemic insult than adults. Thus, NAPE level might be useful as a neurodegenerative marker [38].

We used this post-decapitative brain ischemic model since the remarkable accumulation of NAPEs/NAEs in this model has been reported by several researchers [17,18,22,23] and since the procedure is quite simple and highly reproducible. However, considering that the fluctuations in NAPE/NAE tone almost reflect postmortem change and may not be ascribed solely to ischemia, further analysis of *Pla2g4e*$^{-/-}$ mice is required by using an in vivo model of ischemia-reperfusion as previously reported [36,38,39].

In the current study, we have focused on the brain tissues, and it remains unclear if other tissues show age-dependent changes of cPLA$_2\varepsilon$ as seen in the brain. Previously, using a catalytically inactive mutant, cPLA$_2\varepsilon$ was found to be essential in the endo/lysosomal system in HeLa cells to recycle major histocompatibility complex-1 receptor back to the host cell surface [40]. Thus, *Pla2g4e*$^{-/-}$ mice might be useful to investigate the physiological significance of this finding. Interestingly, a single nucleotide variant of cPLA2ε was recently suggested as a risk factor gene for panic disorder in a case-control study [41]. However, this finding was not statistically significant, and it remained unsolved whether cPLA2ε is involved in the pathogenesis of this neuropsychiatric disease. Very recently, the NAPE-forming ability of cPLA$_2\varepsilon$ was shown to be protective against skin inflammation such as psoriasis by analyzing *Pla2g4e*$^{-/-}$ mice. Consistently, the challenge of the cultured keratinocytes with psoriatic cytokines up-regulated cPLA$_2\varepsilon$ leading to the enhanced NAE production, while the supplementation with NAEs decreased a psoriatic marker [15].

In conclusion, by using *Pla2g4e*$^{-/-}$ mice we showed that cPLA$_2\varepsilon$ is principally responsible for the postmortem production of NAPEs in the brain for the first time. As for NAEs, we suggested that the generations of quantitatively major PEA and OEA largely depended on cPLA$_2\varepsilon$, while those of AEA and DHEA did not. We also suggested the presence of alternative enzyme(s) other than cPLA$_2\varepsilon$ to maintain the basal level of NAPEs. Thus, these results strongly suggest the central role of cPLA$_2\varepsilon$ in the formation of NAPEs and NAEs in the brain on demand like ischemia, but also highlight the involvement of other enzymes to maintain their basal levels.

Funding sources

This work was supported by Grants-in-Aid for Scientific Research (JP19K23828 to Z.H., JP20H05691 to M.M., and JP19K07353 to N.U.) from the Japan Society for the Promotion of Science; Strategic Research Support Fund of Kagawa University Research Promotion Program 2021 (KURPP) (to T.U.); Charitable Trust MIU Foundation Memorial Fund (to T.U.); Takeda Science Foundation (to T.U.); and AMED-CREST JP22gm1210013 (to M.M.) from the Japan Agency for Medical Research and Development.

CRediT authorship contribution statement

S. M. Khaledur Rahman: Investigation, Visualization, Writing - Original Draft, Funding acquisition

Zahir Hussain: Investigation, Visualization, Writing - Original Draft, Funding acquisition

Katsuya Morito: Formal analysis, Investigation, Visualization

Naoko Takahashi: Formal analysis, Investigation

Mohammad Mamun Sikder: Investigation

Tamotsu Tanaka: Project administration

Kenichi Ota: Investigation

Masaki Ueno: Investigation, Visualization, Project administration

Hiroo Takahashi: Investigation

Tohru Yamamoto: Project administration

Makoto Murakami: Resources, Funding acquisition

Toru Uyama: Conceptualization, Investigation, Writing - Original Draft, Project administration, Funding acquisition

Natsuo Ueda: Conceptualization, Writing - Original Draft, Supervision, Project administration, Funding acquisition

Declaration of competing interest

The authors declare that they have no known competing financial interests or personal relationships that could have appeared to influence the work reported in this paper.

Data availability

Data will be made available on request.

Acknowledgements

We acknowledge technical assistance from the Divisions of Research Instrument and Equipment, Animal Experiment and Radioisotope Research, Life Science Research Center, Kagawa University.

Appendix A. Supplementary data

Supplementary data to this article can be found online at https://doi.org/10.1016/j.bbalip.2022.159222.

References

[1] D.E. Epps, V. Natarajan, P.C. Schmid, H.H.O. Schmid, Accumulation of *N*-acylethanolamine glycerophospholipids in infarcted myocardium, Biochim. Biophys. Acta 618 (1980) 420–430, https://doi.org/10.1016/0005-2760(80)90260-X.

[2] H.H.O. Schimd, P.C. Schimd, V. Natarajan, *N*-acylated glycerophospholipids and their derivatives, Prog. Lipid Res. 29 (1990) 1–43, https://doi.org/10.1016/0163-7827(90)90004-5.

[3] N. Wellner, T.A. Diep, C. Janfelt, H.S. Hansen, *N*-acylation of phosphatidylethanolamine and its biological functions in mammals, Biochim. Biophys. Acta 1831 (2013) 652–662, https://doi.org/10.1016/j.bbalip.2012.08.019.

[4] M. Alhouayek, G.G. Muccioli, Harnessing the anti-inflammatory potential of palmitoylethanolamide, Drug Discov. Today 19 (2014) 1632–1639, https://doi.org/10.1016/j.drudis.2014.06.007.

[5] J.D. Brown, E.K. Azari, J.E. Ayala, Oleoylethanolamide : a fat ally in the fight against obesity, Physiol. Behav. 176 (2017) 50–58, https://doi.org/10.1016/j.physbeh.2017.02.034.

[6] F.A. Iannotti, V. Di Marzo, S. Petrosino, Endocannabinoids and endocannabinoid-related mediators: targets, metabolism and role in neurological disorders, Prog. Lipid Res. 62 (2016) 107–128, https://doi.org/10.1016/j.plipres.2016.02.002.

[7] H.-Y. Kim, A.A. Spector, Z.-M. Xiong, A synaptogenic amide *N*-docosahexaenoylethanolamide promotes hippocampal development, Prostaglandins Other Lipid Mediat. 96 (2011) 114–120, https://doi.org/10.1016/j.prostaglandins.2011.07.002.

[8] S.M.K. Rahman, T. Uyama, Z. Hussain, N. Ueda, Roles of endocannabinoids and endocannabinoid-like molecules in energy homeostasis and metabolic regulation: a nutritional perspective, Annu. Rev. Nutr. 41 (2021) 177–202, https://doi.org/10.1146/annurev-nutr-043020-090216.

[9] Y. Okamoto, J. Morishita, K. Tsuboi, T. Tonai, N. Ueda, Molecular characterization of a phospholipase D generating anandamide and its congeners, J. Biol. Chem. 279 (2004) 5298–5305, https://doi.org/10.1074/jbc.M306642200.

[10] K. Tsuboi, Y. Okamoto, N. Ikematsu, M. Inoue, Y. Shimizu, T. Uyama, J. Wang, D. G. Deutsch, M.P. Burns, N.M. Ulloa, A. Tokumura, N. Ueda, Enzymatic formation of *N*-acylethanolamines from *N*-acylethanolamine plasmalogen through *N*-acylphosphatidylethanolamine-hydrolyzing phospholipase D-dependent and -independent pathways, Biochim. Biophys. Acta 1811 (2011) 565–577, https://doi.org/10.1016/j.bbalip.2011.07.009.

[11] Z. Hussain, T. Uyama, K. Tsuboi, N. Ueda, Mammalian enzymes responsible for the biosynthesis of *N*-acylethanolamines, Biochim. Biophys. Acta 1862 (2017) 1546–1561, https://doi.org/10.1016/j.bbalip.2017.08.006.

[12] Y. Ogura, W.H. Parsons, S.S. Kamat, B.F. Cravatt, A calcium-dependent acyltransferase that produces *N*-acyl phosphatidylethanolamines, Nat. Chem. Biol. 12 (2016) 669–671, https://doi.org/10.1038/nchembio.2127.

[13] S.S. Binte Mustafiz, T. Uyama, K. Morito, N. Takahashi, K. Kawai, Z. Hussain, K. Tsuboi, N. Araki, K. Yamamoto, T. Tanaka, N. Ueda, Intracellular Ca^{2+}-dependent formation of *N*-acyl-phosphatidylethanolamines by human cytosolic phospholipase $A_{2\varepsilon}$, Biochim. Biophys. Acta 1864 (2019), 158515 https://doi.org/10.1016/j.bbalip.2019.158515.

[14] Z. Hussain, T. Uyama, K. Kawai, S.S. Binte Mustafiz, K. Tsuboi, N. Araki, N. Ueda, Phosphatidylserine-stimulated production of *N*-acyl-phosphatidylethanolamines by Ca^{2+}-dependent *N*-acyltransferase, Biochim. Biophys. Acta 1863 (2018) 493–502, https://doi.org/10.1016/j.bbalip.2018.02.002.

[15] L. Liang, R. Takamiya, Y. Miki, K. Heike, Y. Taketomi, N. Sugimoto, M. Yamaguchi, H. Shitara, Y. Nishito, T. Kobayashi, T. Hirabayashi, M. Murakami, Group IVE cytosolic phospholipase A_2 limits psoriatic inflammation by mobilizing the anti-inflammatory lipid *N*-acylethanolamine, FASEB J. 36 (2022), e22301, https://doi.org/10.1096/fj.202101958R.

[16] H.S. Hansen, B. Moesgaard, H.H. Hansen, G. Petersen, *N*-acylethanolamines and precursor phospholipids — relation to cell injury, Chem. Phys. Lipids 108 (2000) 135–150, https://doi.org/10.1016/S0009-3084(00)00192-4.

[17] V. Natarajan, P.C. Schmid, H.H.O. Schmid, *N*-acylethanolamine phospholipid metabolism in normal and ischemic rat brain, Biochim. Biophys. Acta 878 (1986) 32–41, https://doi.org/10.1016/0005-2760(86)90341-3.

[18] B. Moesgaard, G. Petersen, J.W. Jaroszewski, H.S. Hansen, Age dependent accumulation of *N*-acyl-ethanolamine phospholipids in ischemic rat brain: a ^{31}P NMR and enzyme activity study, J. Lipid Res. 41 (2000) 985–990, https://doi.org/10.1016/S0022-2275(20)32041-1.

[19] Z. Hussain, T. Uyama, K. Kawai, I.A.S. Rahman, K. Tsuboi, N. Araki, N. Ueda, Comparative analyses of isoforms of the calcium-independent phosphatidylethanolamine *N*-acyltransferase PLAAT-1 in humans and mice, J. Lipid Res. 57 (2016) 2051–2060, https://doi.org/10.1194/jlr.M071290.

[20] X. Jin, Y. Okamoto, J. Morishita, K. Tsuboi, T. Tonai, N. Ueda, Discovery and characterization of a Ca^{2+}-independent phosphatidylethanolamine *N*-acyltransferase generating the anandamide precursor and its congeners, J. Biol. Chem. 282 (2007) 3614–3623, https://doi.org/10.1074/jbc.M606369200.

[21] T. Uyama, J. Morishita, X. Jin, Y. Okamoto, K. Tsuboi, The tumor suppressor gene H-Rev107 functions as a novel Ca^{2+}-independent cytosolic phospholipase $A_{1/2}$ of the thiol hydrolase type, J. Lipid Res. 50 (2009) 685–693, https://doi.org/10.1194/jlr.M800453-JLR200.

[22] S. Patel, E.J. Carrier, W.V. Ho, D.J. Rademacher, S. Cunningham, D.S. Reddy, J. R. Falck, B.F. Cravatt, C.J. Hillard, The postmortal accumulation of brain *N*-arachidonylethanolamine (anandamide) is dependent upon fatty acid amide hydrolase activity, J. Lipid Res. 46 (2005) 342–349, https://doi.org/10.1194/jlr.M400377-JLR200.

[23] K. Kempe, F. Hsu, A. Bohrer, J. Turk, Isotope dilution mass spectrometric measurements indicate that arachidonylethanolamide, the proposed endogenous ligand of the cannabinoid receptor, accumulates in rat brain tissue post mortem but is contained at low levels in or is absent from fresh tissue, J. Biol. Chem. 271 (1996) 17287–17295, https://doi.org/10.1074/jbc.271.29.17287.

[24] M. Inoue, K. Tsuboi, Y. Okamoto, M. Hidaka, T. Uyama, T. Tsutsumi, T. Tanaka, N. Ueda, A. Tokumura, Peripheral tissue levels and molecular species compositions of *N*-acyl-phosphatidylethanolamine and its metabolites in mice lacking *N*-acyl-phosphatidylethanolamine-specific phospholipase D, J. Biochem. 162 (2017) 449–458, https://doi.org/10.1093/jb/mvx054.

[25] I.A.S. Rahman, K. Tsuboi, Z. Hussain, R. Yamashita, Y. Okamoto, T. Uyama, N. Yamazaki, T. Tanaka, A. Tokumura, N. Ueda, Calcium-dependent generation of *N*-acylethanolamines and lysophosphatidic acids by glycerophosphodiesterase GDE7, Biochim. Biophys. Acta 1861 (2016) 1881–1892, https://doi.org/10.1016/j.bbalip.2016.09.008.

[26] T. Uyama, M. Inoue, Y. Okamoto, N. Shinohara, T. Tai, K. Tsuboi, T. Inoue, A. Tokumura, N. Ueda, Involvement of phospholipase A/acyltransferase-1 in *N*-acylphosphatidylethanolamine generation, Biochim. Biophys. Acta 1831 (2013) 1690–1701, https://doi.org/10.1016/j.bbalip.2013.08.017.

[27] T. Ohto, N. Uozumi, T. Hirabayashi, T. Shimizu, Identification of novel cytosolic phospholipase A_2s, murine cPLA$_2$δ, ε, and ζ, which form a gene cluster with cPLA$_2$β, J. Biol. Chem. 280 (2005) 24576–24583, https://doi.org/10.1074/jbc.M413711200.

[28] P.C. Schmid, R.J. Krebsbach, S.R. Perry, T.M. Dettmer, J.L. Maasson, H.H. O. Schmid, Occurrence and postmortem generation of anandamide and other long-chain *N*-acylethanolamines in mammalian brain, FEBS Lett. 375 (1995) 117–120, https://doi.org/10.1016/0014-5793(95)01194-J.

[29] B. Moesgaard, J.W. Jaroszewski, H.S. Hansen, Accumulation of *N*-acyl-ethanolamine phospholipids in rat brains during post-decapitative ischemia: a ^{31}P NMR study, J. Lipid Res. 40 (1999) 515–521, https://doi.org/10.1016/S0022-2275(20)32456-1.

[30] D. Leung, A. Saghatelian, G.M. Simon, B.F. Cravatt, Inactivation of *N*-acyl phosphatidylethanolamine phospholipase D reveals multiple mechanisms for the biosynthesis of endocannabinoids, Biochemistry 45 (2006) 4720–4726, https://doi.org/10.1021/bi060163l.

[31] B.L. Sabatini, T.G. Oertner, K. Svoboda, The life cycle of Ca^{2+} ions in dendritic spines, Neuron 33 (2002) 439–452, https://doi.org/10.1016/S0896-6273(02)00573-1.

[32] C.C. Leslie, Regulation of the specific release of arachidonic acid by cytosolic phospholipase A_2, Prostaglandins, Leukot. Essent. Fat. Acids. 70 (2004) 373–376, https://doi.org/10.1016/j.plefa.2003.12.012.

[33] B.F. Cravatt, D.K. Giang, S.P. Mayfield, D.L. Boger, R.A. Lerner, N.B. Gilula, Molecular characterization of an enzyme that degrades neuromodulatory fatty-acid amides, Nature 384 (1996) 83–87, https://doi.org/10.1038/384083a0.

[34] N. Ueda, Y. Kurahashi, S. Yamamoto, T. Tokunaga, Partial purification and characterization of the porcine brain enzyme hydrolyzing and synthesizing anandamide, J. Biol. Chem. 270 (1995) 23823–23827, https://doi.org/10.1074/jbc.270.40.23823.

[35] F. Palese, S. Pontis, N. Realini, D. Piomelli, A protective role for *N*-acylphosphatidylethanolamine phospholipase D in 6-OHDA-induced neurodegeneration, Sci. Rep. 9 (2019) 15927, https://doi.org/10.1038/s41598-019-51799-1.

[36] A. Kilaru, P. Tamura, P. Garg, G. Isaac, D. Baxter, S. Duncan, R. Welti, P. Koulen, K. D. Chapman, B.J. Venables, Changes in *N*-acylethanolamine pathway related metabolites in a rat model of cerebral ischemia/reperfusion, J. Glycomics Lipidomics 1 (2011) 101. http://www.ncbi.nlm.nih.gov/pmc/articles/pmc4457465/.

[37] Y. Sun, S.P.H. Alexander, M.J. Garle, C.L. Gibson, K. Hewitt, S.P. Murphy, D. A. Kendall, A.J. Bennett, Cannabinoid activation of PPARα; a novel neuroprotective mechanism, Br. J. Pharmacol. 152 (2007) 734–743, https://doi.org/10.1038/sj.bjp.0707478.

[38] D. Luptakova, L. Baciak, T. Pluhacek, A. Skriba, B. Sediva, V. Havlicek, I. Juranek, Membrane depolarization and aberrant lipid distributions in the neonatal rat brain following hypoxic-ischaemic insult, Sci. Rep. 8 (2018) 6952, https://doi.org/10.1038/s41598-018-25088-2.

[39] C. Janfelt, N. Wellner, P.L. Leger, J. Kokesch-Himmelreich, S.H. Hansen, C. Charriaut-Marlangue, H.S. Hansen, Visualization by mass spectrometry of 2-dimensional changes in rat brain lipids, including *N*-acylphosphatidylethanolamines, during neonatal brain ischemia, FASEB J. 26 (2012) 2667–2673, https://doi.org/10.1096/fj.11-201152.

[40] M. Capestrano, S. Mariggio, G. Perinetti, A.V. Egorova, S. Iacobacci, M. Santoro, A. Di Pentima, C. Iurisci, M.V. Egorov, G. Di Tullio, R. Buccione, A. Luini, R. S. Polishchuk, Cytosolic phospholipase $A_2\varepsilon$ drives recycling through the clathrin-independent endocytic route, J. Cell Sci. 127 (2014) 977–993, https://doi.org/10.1242/jcs.136598.

[41] Y. Morimoto, M. Shimada-sugimoto, T. Otowa, S. Yoshida, A. Kinoshita, H. Mishima, N. Yamaguchi, T. Mori, A. Imamura, H. Ozawa, N. Kurotaki, C. Ziegler, K. Domschke, J. Deckert, T. Umekage, M. Tochigi, H. Kaiya, Y. Okazaki, K. Tokunaga, T. Sasaki, K. Yoshiura, S. Ono, Whole-exome sequencing and gene-based rare variant association tests suggest that PLA2G4E might be a risk gene for panic disorder, Transl. Psychiatry 8 (2018) 41, https://doi.org/10.1038/s41398-017-0088-0.

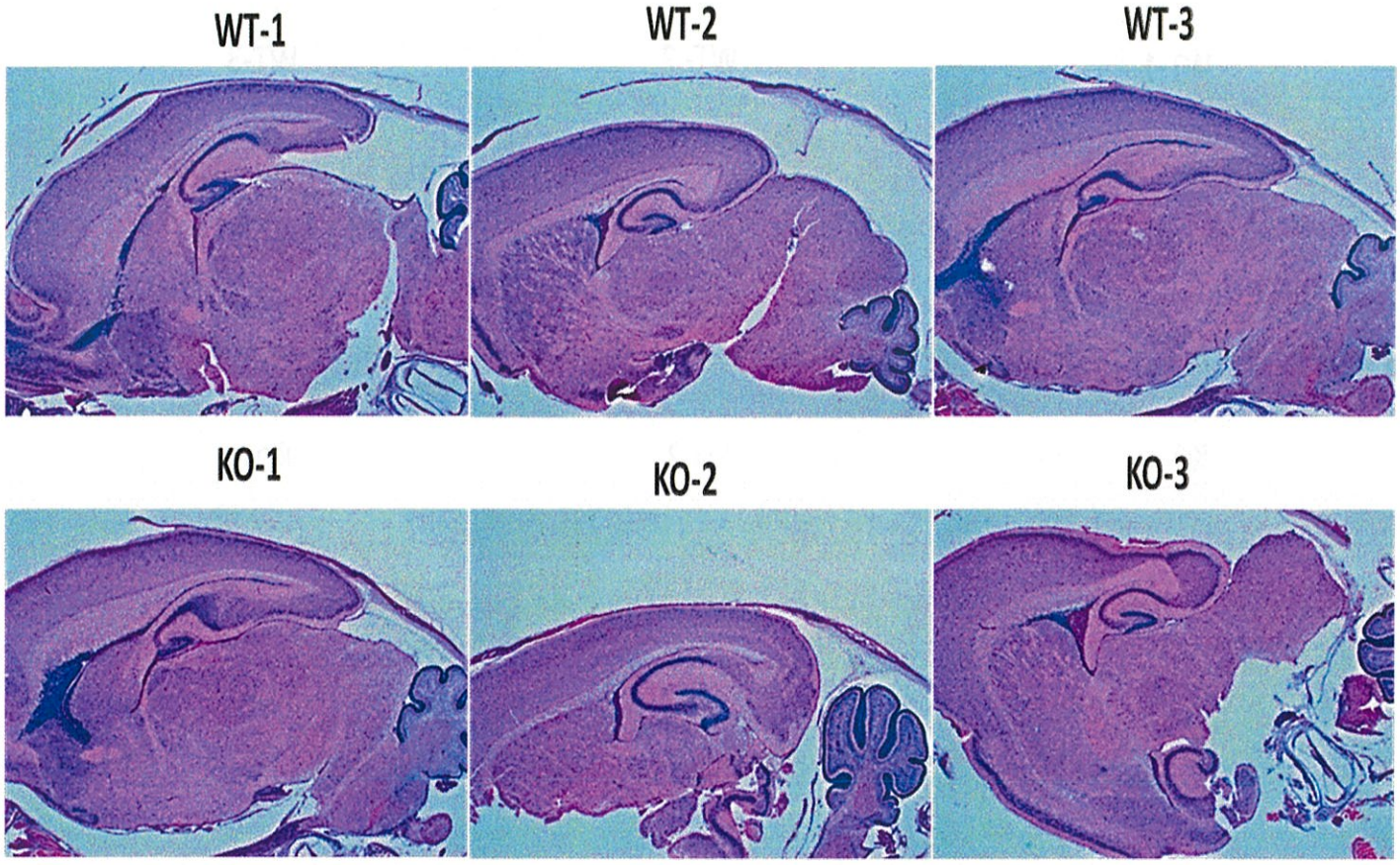

Supplementary Figure 1

Hematoxylin and eosin staining in three WT mice and three *Pla2g4e*$^{-/-}$ (KO) mice at P7.

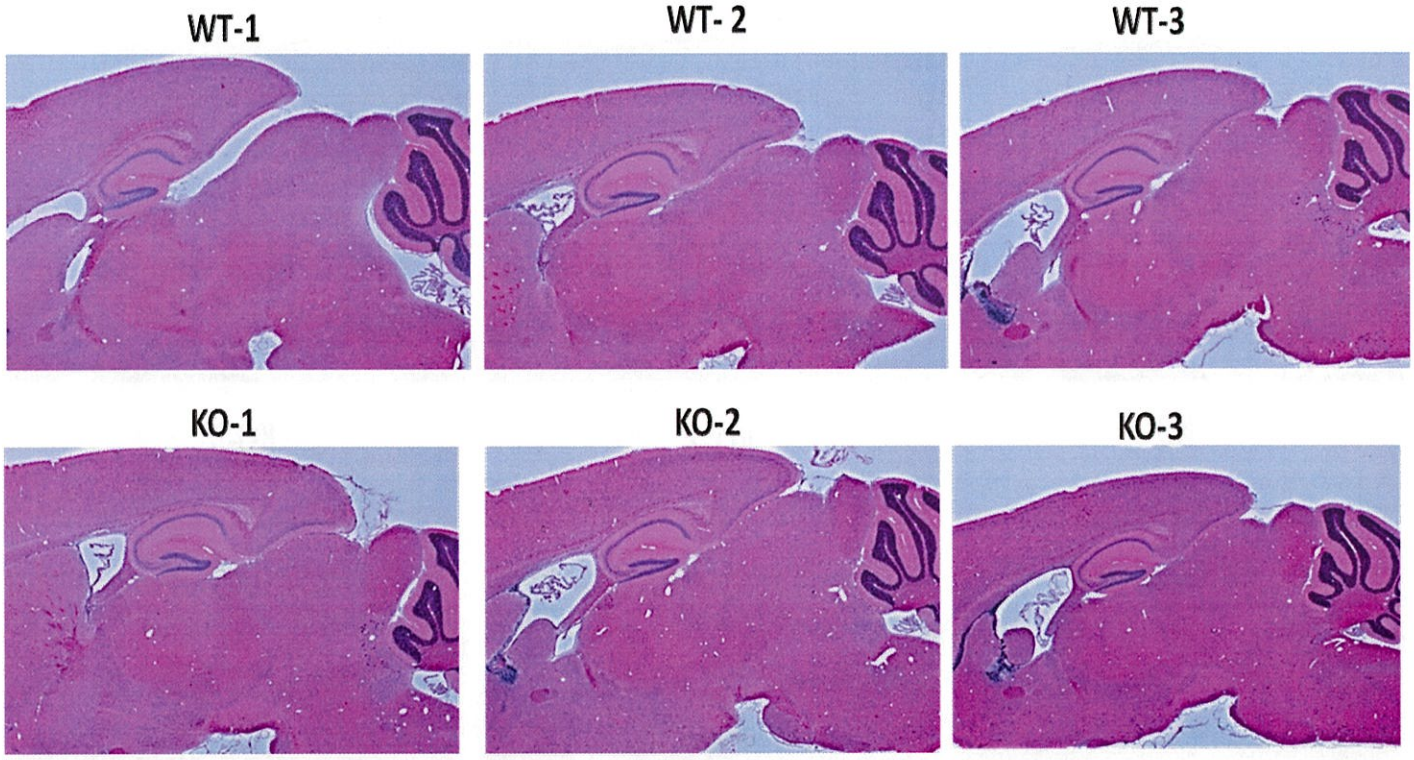

Supplementary Figure 2

Hematoxylin and eosin staining in three WT mice and three *Pla2g4e*$^{-/-}$ (KO) mice at P30.

Supplementary table 1. Post-decapitative accumulation of total NAPEs and NAEs in the brains of WT and *Pla2g4e*$^{-/-}$ (KO) mice

		WT			KO		
		0 h (nmol/g tissue)	**6 h** (nmol/g tissue)	**Fold change (6 h/ 0 h)**	**0 h** (nmol/g tissue)	**6 h** (nmol/g tissue)	**Fold change (6 h/ 0 h)**
NAPE	**Diacyl**	0.329	6.751	20.5	0.253	0.324	1.3
	Alkenylacyl	0.363	3.08	8.5	0.191	0.19	1.0
NAE		0.887	194.376	219.1	0.683	5.912	8.7

Supplementary table 2. Post-decapitative accumulation of various diacyl species of NAPEs in WT and *Pla2g4e*$^{-/-}$ (KO) mouse brains

		WT			KO		
R_2CO	$R_1CO + R_NCO$	**0 h** (nmol/g tissue)	**6 h** (nmol/g tissue)	**Fold change (6 h/ 0 h)**	**0 h** (nmol/g tissue)	**6 h** (nmol/g tissue)	**Fold change (6 h/ 0 h)**
18:1	32:1	0.008	0.188	23.5	0.004	0.019	4.8
	32:0	0.029	0.849	29.3	0.022	0.046	2.1
	34:2	0.008	0.077	9.6	0.006	0.007	1.2
	34:1	0.036	0.421	11.7	0.022	0.031	1.4
	34:0	0.031	0.939	30.3	0.027	0.035	1.3
	36:2	0.018	0.096	5.3	0.014	0.009	0.6
	36:1	0.025	0.275	11.0	0.019	0.022	1.2
	36:0	0.053	0.615	11.6	0.042	0.046	1.1
	38:5	0.009	0.203	22.6	0.009	0.007	0.8
	38:4	0.008	0.42	52.5	0.007	0.008	1.1
	38:2	0.007	0.057	8.1	0.006	0.008	1.3
	38:1	0.009	0.075	8.3	0.008	0.010	1.3
	38:0	0.021	0.098	4.7	0.011	0.010	0.9
	40:8	0.005	0.062	12.4	0.005	0.005	1.0
	40:4	0.009	0.102	11.3	0.014	0.010	0.7
	40:2	0.012	0.055	4.6	0.008	0.008	1.0
	40:1	0.010	0.031	3.1	0.009	0.009	1.0
	42:10	0.004	0.010	2.5	0.006	0.004	0.7
18:2	34:0	0.004	0.109	27.3	0.003	0.003	1.0
20:4	34:0	0.030	2.144	71.5	0.019	0.038	2.0

Supplementary table 3. Post-decapitative accumulation of various alkenylacyl species of NAPEs in WT and *Pla2g4e*$^{-/-}$ (KO) mouse brains

		WT			KO		
R_2CO	$R_1(CH)_2+R_NCO$	**0 h** (nmol/g tissue)	**6 h** (nmol/g tissue)	**Fold change (6 h/ 0 h)**	**0 h** (nmol/g tissue)	**6 h** (nmol/g tissue)	**Fold change (6 h/ 0 h)**
18:1	32:1	0.015	0.134	8.9	0.015	0.021	1.4
	34:2	0.013	0.066	5.1	0.008	0.008	1.0
	34:1	0.036	0.203	5.6	0.015	0.025	1.7
	36:3	0.033	0.033	1.0	0.012	0.009	0.8
	36:2	0.02	0.039	2.0	0.007	0.01	1.4
	36:1	0.015	0.069	4.6	0.009	0.017	1.9
	38:7	0.083	1.131	13.6	0.049	0.04	0.8
	38:6	0.08	0.622	7.8	0.04	0.03	0.8
	38:2	0.006	0.006	1.0	0.002	0.003	1.5
	40:8	0.024	0.115	4.8	0.013	0.01	0.8
	40:2	0.003	0.013	4.3	0.002	0.002	1.0
	42:2	0.01	0.05	5.0	0.006	0.003	0.5
20:4	34:1	0.025	0.6	24.0	0.012	0.016	1.3

Supplementary table 4. Post-decapitative accumulation of various species of NAEs in WT and *Pla2g4e*$^{-/-}$ (KO) mouse brains

	WT			KO		
R_NCO	**0 h** (nmol/g tissue)	**6 h** (nmol/g tissue)	**Fold change (6 h/ 0 h)**	**0 h** (nmol/g tissue)	**6 h** (nmol/g tissue)	**Fold change (6 h/ 0 h)**
16:0	0.268	105	392.0	0.24	3.185	13.3
16:1	0.04	8.064	201.6	0.054	0.246	4.6
18:0	0.19	39.43	208.0	0.026	0.489	18.8
18:1	0.281	29.02	104.0	0.242	1.302	5.4
18:2	0.027	2.72	100.7	0.046	0.172	3.7
18:3	5.00E-04	0.045	90.0	4.00E-04	0.008	20.0
20:0	0.007	0.025	3.6	0	0.001	ND
20:1	0.006	0.983	163.8	8.00E-04	0.018	22.5
20:2	0.013	1.599	123.0	0.011	0.068	6.2
20:3	0.007	1.559	222.7	0.007	0.125	17.9
20:4	0.015	0.944	64.0	0.027	0.768	29.0
20:5	0	0.018	ND	2.00E-04	0.011	55.0
22:1	0.005	0.007	1.4	0	0	ND
22:2	6.00E-04	0.024	40.0	0	6.00E-04	ND
22:3	0.003	0.483	161.0	0.001	0.012	12.0
22:4	0.01	4.327	432.7	0.008	0.062	7.8
22:5	0.001	0.768	768.0	0.002	0.019	9.5
22:6	0.029	0.283	10.0	0.045	0.192	4.3

ND, not determined due to 0 value of denominators